



**Geological Survey
of Canada**

**CURRENT RESEARCH
2002-F3**

**SHRIMP U-Pb ages of multiple metamorphic
events in the Angikuni Lake area, western
Churchill Province, Nunavut**

*Robert G. Berman, William J. Davis, Lawrence B. Aspler,
and Jeffrey R. Chiarenzelli*

2002



Natural Resources
Canada

Ressources naturelles
Canada

Canada

©Her Majesty the Queen in Right of Canada 2002
ISSN No. 1701-4387

Available in Canada from the
Geological Survey of Canada Bookstore website at:
<http://www.nrcan.gc.ca/gsc/bookstore> (Toll-free: 1-888-252-4301)

A copy of this publication is also available for reference by depository
libraries across Canada through access to the Depository Services Program's
website at <http://dsp-psd.pwgsc.gc.ca>

Price subject to change without notice

All requests for permission to reproduce this work, in whole or in part, for purposes of commercial use, resale, or redistribution shall be addressed to: Earth Sciences Sector Information Division, Room 402, 601 Booth Street, Ottawa, Ontario K1A 0E8.

Authors' addresses

R.G. Berman (rberman@nrcan.gc.ca)

W.J. Davis (bidavis@nrcan.gc.ca)

Continental Geoscience Division

Geological Survey of Canada

601 Booth Street

Ottawa, Ontario K1A 0E8

L.B. Aspler (nwtgeol@sympatico.ca)

23 Newton St.

Ottawa, Ontario K1S 2S6

J.R. Chiarenzelli (chiarejr@potdam.edu)

Department of Geology, State University of New York

at Potsdam

Potsdam, New York

USA 13676

Publication approved by Continental Geoscience Division

SHRIMP U-Pb ages of multiple metamorphic events in the Angikuni Lake area, western Churchill Province, Nunavut¹

Robert G. Berman, William J. Davis, Lawrence B. Aspler,
and Jeffrey R. Chiarenzelli

Berman, R.G., Davis, W.J., Aspler, L.B., and Chiarenzelli, J.R., 2002: SHRIMP U-Pb ages of multiple metamorphic events in the Angikuni Lake area, western Churchill Province, Nunavut; Radiogenic Age and Isotopic Studies: Report 15; Geological Survey of Canada, Current Research 2002-F3, 9 p.

Abstract: Paragneiss near Angikuni Lake, Nunavut contains large, low-CaO garnet porphyroblasts (type I), enveloped by gneissic layering, and post-tectonic, thin garnet rims and microporphyroblasts with much higher CaO (type II). Calculated pressure-temperature conditions are approximately 5.4 kbar and 730°C for type I garnet, and 11 kbar and 740°C for type II garnet. In situ sensitive high-resolution ion microprobe (SHRIMP) measurements yielded two age populations of monazite, 2.54 ± 0.02 Ga and 1.93 ± 0.05 Ga, that are interpreted to date the two types of garnet growth. The new data indicate that a domain of 2.56–2.5 Ga high-grade metamorphism and associated deformation extends approximately 400 km from Chesterfield Inlet at least as far southwest as the Angikuni Lake area.

Résumé : Dans des paragneiss situés près du lac Angikuni (Nunavut), on observe de gros porphyroblastes de grenat à faible teneur en CaO (type I), qui sont enveloppés par le rubanement gneissique, ainsi que des grenats post-tectoniques à plus forte teneur en CaO (type II), lesquels forment de minces bordures sur des cristaux plus anciens ou constituent des microporphyroblastes. Les conditions de température-pression calculées sont d'environ 730 °C – 5,4 kbar pour les grenats de type I et de 740 °C – 11 kbar pour les grenats de type II. Les datations réalisées par des mesures localisées à la microsonde ionique à haute résolution et haut niveau de sensibilité (SHRIMP) sur des cristaux de monazite définissent deux populations, l'une située à $2,54 \pm 0,02$ Ga et l'autre à $1,93 \pm 0,05$ Ga. Ces deux valeurs rendraient compte des épisodes de croissance des deux types de grenat. Les nouvelles données permettent de définir un domaine marqué par les effets d'un métamorphisme de degré élevé et d'une déformation associée à 2,56-2,5 Ga. Celui-ci s'étend sur environ 400 km en direction du sud-ouest, depuis la baie Chesterfield jusqu'à la région du lac Angikuni et même au-delà.

¹ Contribution of the Western Churchill NATMAP Project

INTRODUCTION

The Rae and Hearne domains of the western Churchill Province (Fig. 1) constitute a heterogeneously reworked Archean craton that represents the upper plate to both the ca. 1.97–1.91 Ga Thelon–Taltson Orogen (Hoffman, 1990) and the 1.83–1.78 Ga terminal stage of the Trans-Hudson Orogen (Ansdell et al., 1995). It has long been surmised, from widespread K–Ar ages of less than 1.75 Ga (e.g. Davidson, 1972; Stockwell, 1982), that much of the western Churchill Province experienced Hudsonian reworking, at least at low metamorphic grade. There have, however, been very few direct determinations of peak metamorphic ages that can be used to distinguish between the effects of different Paleoproterozoic and Archean events.

Recent work has revealed that prominent metamorphic events at ca. 2.56–2.50 Ga and 1.9 Ga have variably affected supracrustal rocks at Parker Lake–MacQuoid Lake (Fig. 2; Berman et al., 2000; Stern and Berman, 2000) and Yathkyed Lake (MacLachlan et al., 2000), as well as granulite-facies rocks at deeper structural levels within the Kramanituar complex (Sanborn-Barrie et al., 2001), Uvauk complex (Tella et al., 1994; Mills, 2001), and Big Lake shear zone (Ryan et al., 2000). The recognition of a regional, ca. 2.5 Ga tectonometamorphic event led, in part, to the suggestion of a distinct ‘northwestern Hearne domain’ (Davis et al., 2000),

but definition of the extent and boundaries of the region affected by both the 2.56–2.50 Ga and 1.9 Ga events remains a significant problem. This paper provides metamorphic and geochronological data for a high-grade metamorphic rock from Angikuni Lake (Fig. 2). The results indicate that this sample has experienced the same style and timing of metamorphic events as the Parker Lake–MacQuoid Lake supracrustal belt, thereby establishing a link that warrants southwestward expansion of the northwestern Hearne domain to include parts of the Angikuni Lake area.

GEOLOGICAL SETTING

Angikuni Lake straddles the central segment of the Snowbird tectonic zone, the geophysically defined boundary between the Hearne and Rae domains of the western Churchill Province (Fig. 1, 2; Hoffman, 1990). The Neoproterozoic rocks define seven lithostructural domains cut by a network of shear zones (Fig. 3; Aspler et al., 1999 and references therein). Two of these (domains 1 and 3) contain extensive greenschist- to amphibolite-grade, ca. 2.69–2.68 Ga supracrustal rocks. The remainder consist of upper-amphibolite-grade gneiss and variably deformed gabbroic to granitic intrusions. This paper presents metamorphic and geochronological data for one sample (z6858) from the central part of domain 2.

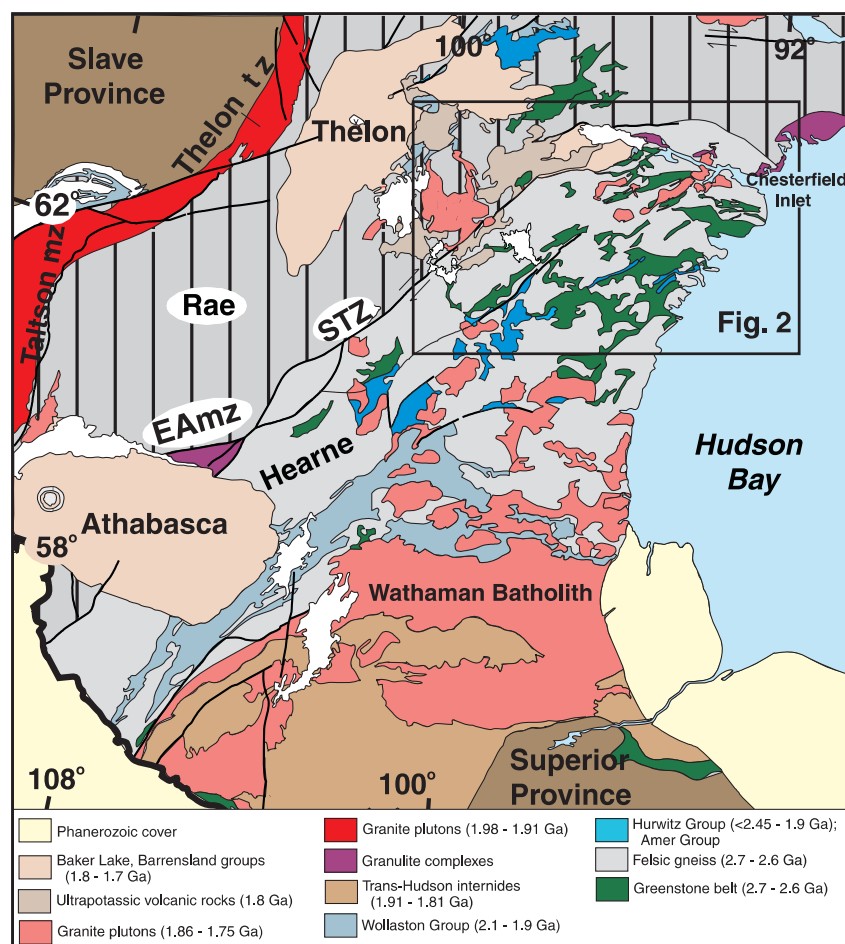


Figure 1.

Regional geology of part of the western Churchill Province, showing the Rae and Hearne domains (modified after Wheeler et al., 1996). EAmz, East Athabasca mylonite zone; STZ, Snowbird tectonic zone; tz, tectonic zone; mz, magmatic zone.

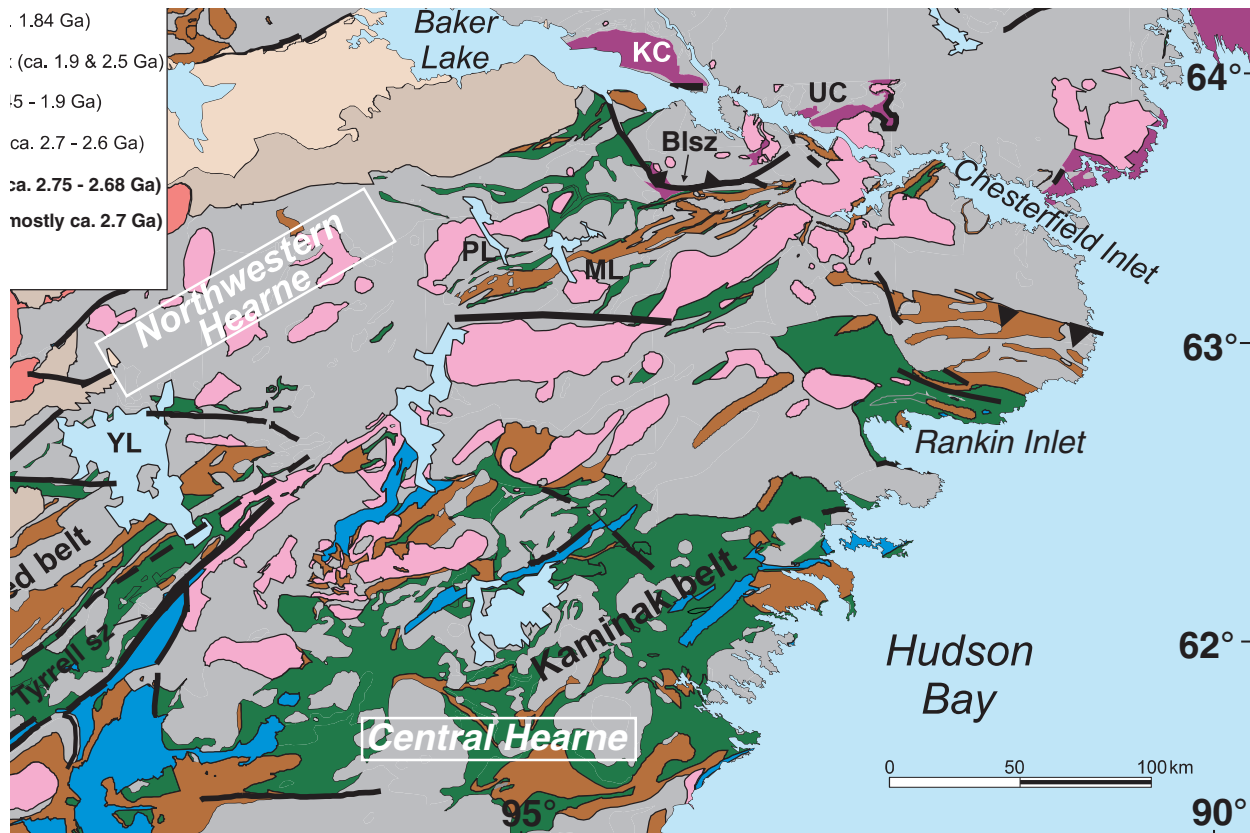


Figure 2. Regional geology of the western Churchill Province in the vicinity of the Rae–Hearne boundary (modified after Paul et al., in press). AL, Angikuni Lake; BLsz, Big Lake shear zone; KC, Kramanitar complex; ML, MacQuoid Lake; PL, Parker Lake; UC, Uvauk complex; YL, Yathkyed Lake. Polygon at lower left shows area of Figure 3.

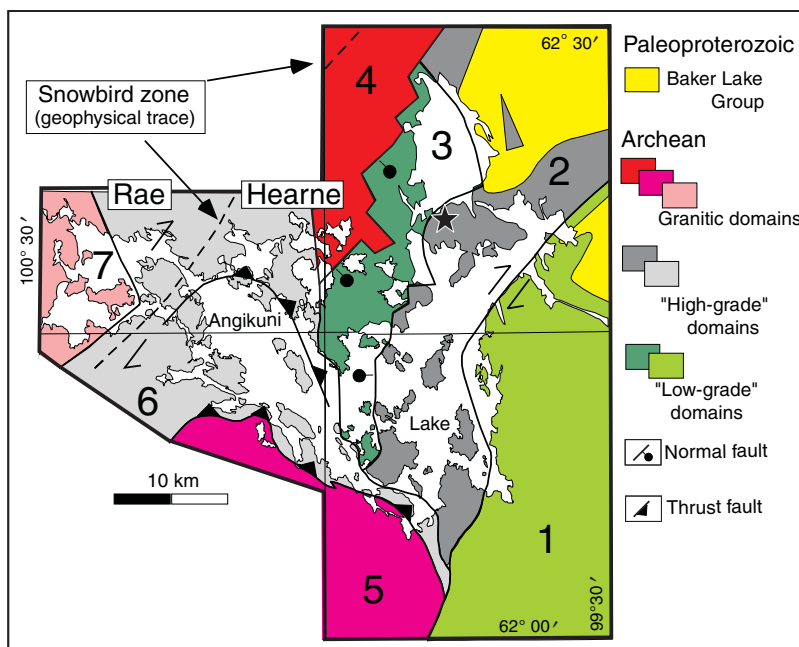


Figure 3.

Lithostructural domains in the vicinity of Angikuni Lake. Star indicates location of sample z6858.

Domain 2 is a complex of upper-amphibolite-grade granite, gabbro, orthogneiss, and paragneiss (Aspler et al., 1999 and references therein). Supracrustal gneissic rocks are the oldest recognizable components. These occur within granitic plutonic rocks and derived gneissic rocks, and range in scale from mappable screens, to metre-scale layers, to partially assimilated xenoliths. Multiple generations of tonalitic to granitic neosome occur in the paragneiss, and range from foliation-parallel lenses to crosscutting injections. The amount of neosome varies from a few per cent to extensive layers. Zones in which partially assimilated enclaves are engulfed by leucosomal material grade to granitic gneiss with decreasing enclave abundance. Swirly gneissosity patterns appear in outcrops due to complex interference between granitic neosome and enclaves, and deflection around variably oriented gabbroic and granitic bodies. Sample z6858 (field no. 97LA-10-10) is from a large (hundreds of metres) enclave of mixed psammitic and pelitic gneiss that displays layering defined by alternating garnet-rich and garnet-poor zones, similar to that illustrated in Figure 4a.

Amphibolite-grade mylonitic rocks and younger greenschist-grade cataclasite are distributed throughout Angikuni Lake and continue across the trace of the Snowbird tectonic zone. The boundary between domains 1 and 2 is an approximately 0.5 km wide, near-vertical, upper-amphibolite-grade, mylonitic, dextral shear zone. Early dextral strike-slip movement predates ca. 2.61 Ga, with continued fabric development after ca. 2.61 Ga (K. MacLachlan and W. Davis, unpub. data, 2002). The boundary between domain 2 and low-grade supracrustal rocks of domain 3 is marked by short fault segments with north, northwest and northeast trends. Some of these faults define near-vertical zones of greenschist-grade granitic cataclasite.

METAMORPHISM

Paragneiss sample z6858 contains the assemblage garnet–biotite–plagioclase–potassium feldspar–quartz–apatite–pyrite–ilmenite. The rock displays a single strong gneissosity defined by alternating quartzofeldspathic and biotite-rich layers that envelop, and are deflected around, large garnet porphyroblasts up to several centimetres in diameter (type I garnet; Fig. 4b). A second generation of garnet (type II) with distinct chemistry occurs as microporphyroblasts (Fig. 4c) and thin rims (Fig. 4d), both less than 0.3 mm wide, on type I garnet. Type II garnet grew after gneissosity formation, based on inclusions of elongate quartz aligned parallel to the external fabric (Fig. 4d), as well as the lack of evidence of gneissic layering deflecting around type II garnet (Fig. 4c). Both garnet types may be partially broken down to small mats of randomly oriented biotite laths, which themselves are partly chloritized.

Mineral compositions (Table 1) were obtained using procedures described by Berman and Bostock (1997). The main chemical contrast between garnet types is the markedly higher CaO content of type II garnet rims and microporphyroblasts (Fig. 4c, 4d). Type I garnet is characterized by mole fraction of grossular (X_{Grs}) < 0.05, except for the outer 70–80 μm of garnet cores, which typically increase to X_{Grs} = 0.063–0.067 (left side of Fig. 5a). One side of the chemical profile (right side of Fig. 5a) shows that CaO increases up to X_{Grs} = 0.114 before dropping by 0.01 at the extreme edge of the type I garnet core. Type II garnet rims display an outward increase in CaO (up to X_{Grs} = 0.18–0.24), before decreasing at their outer rims. Qualitative Ca concentration maps show that fractures approximately 0.2–0.3 mm inboard of the type I garnet rims also have elevated CaO levels similar to those in

Table 1. Thermobarometric data and mineral compositions for sample z6858.

P-T ¹	Type II Garnet (Grt)				Type I Garnet (Grt)			
	<12.1 ² - 750 (eqa. 2,1) >9.8 ³ - 740 (eqa. 3,1) } 11 - 750				<5.6 ² - 730 (eqa. 2,1) >5.2 ³ - 730 (eqa. 3,1) } 5.4 - 730			
	Grt ^{II}	Bt ^m	Plg ^m	Opx ³	Grt ^I	Bt ^m	Plg ^m	Opx ³
Na ₂ O	-	-	7.80	-	-	-	7.70	-
K ₂ O	0.02	9.1	0.20	-	0.01	9	0.50	-
FeO	30.02	16.90	0.1	28.80	25.57	14.8	0.10	27.60
MgO	6.88	10.40	-	17.00	4.94	13.8	-	18.20
CaO	1.73	-	6.6	0.1	8.75	-	6.3	0.10
MnO	1.12	0.10	-	0.3	0.69	-	-	0.30
SiO ₂	37.99	35.90	59.60	49.7	37.68	36.20	59.7	49.70
TiO ₂	0.02	6.6	-	0.10	0.06	3.80	-	0.10
Al ₂ O ₃	21.37	13.4	24.80	3.20	21.48	14.50	24.7	3.2
Total	99.15	92.40	99.10	99.20	99.18	92.1	99	99.2

¹ calculated with TWQ (v. 1.02) software from intersection of equilibria (1), (2), and (3):
 (1) almandine + phlogopite = pyrope + annite
 (2) 2 almandine + grossular + 2 K-feldspar + 2 H₂O = 3 quartz + 3 anorthite + 2 annite
 (3) 3 ferrosilite + 3 anorthite = 2 almandine + grossular + 3 quartz
² maximum P calculated with $a_{\text{H}_2\text{O}} = 1$
³ minimum P calculated with fictive Fe/(Fe + Mg) in Opx that yields T of equilibrium (1)
 Abbreviations: Grt, garnet; Bt, biotite; Plg, plagioclase; Opx, orthopyroxene; I, Type I garnet; II, Type II garnet; m, matrix

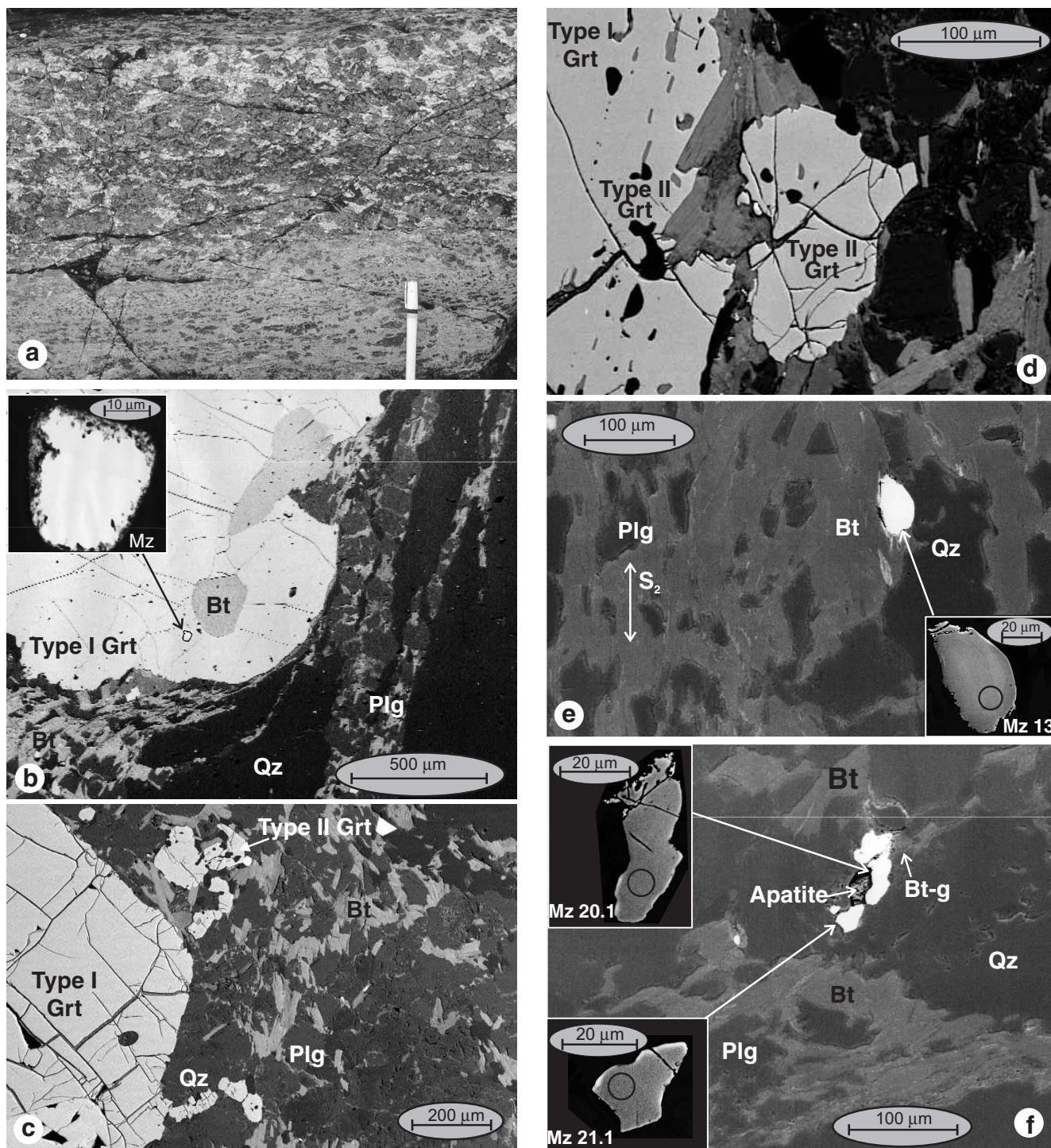


Figure 4. Macroscopic and microscopic (scanning electron microscope) textures of sample z6858: **a)** outcrop photograph of domain 2 mixed psammitic-pelitic gneiss with garnet-rich zone above psammitic layer; **b)** type I garnet enveloped by gneissic layers; inset shows idiomorphic monazite inclusion, interpreted as synmetamorphic, with alteration around margins; **c)** type II garnet microporphyroblasts; **d)** post-tectonic type II garnet forming thin rims with quartz inclusions aligned with matrix fabric; **e)** textural location of ca. 2.54 Ga monazite grain 13; **f)** textural location of ca. 1.93 Ga monazite grains 20 and 21; note monazite truncation of gneissosity-aligned biotite (Bt-g). Bt, biotite; Grt, garnet; Mz, monazite; Plg, plagioclase; Qz, quartz.

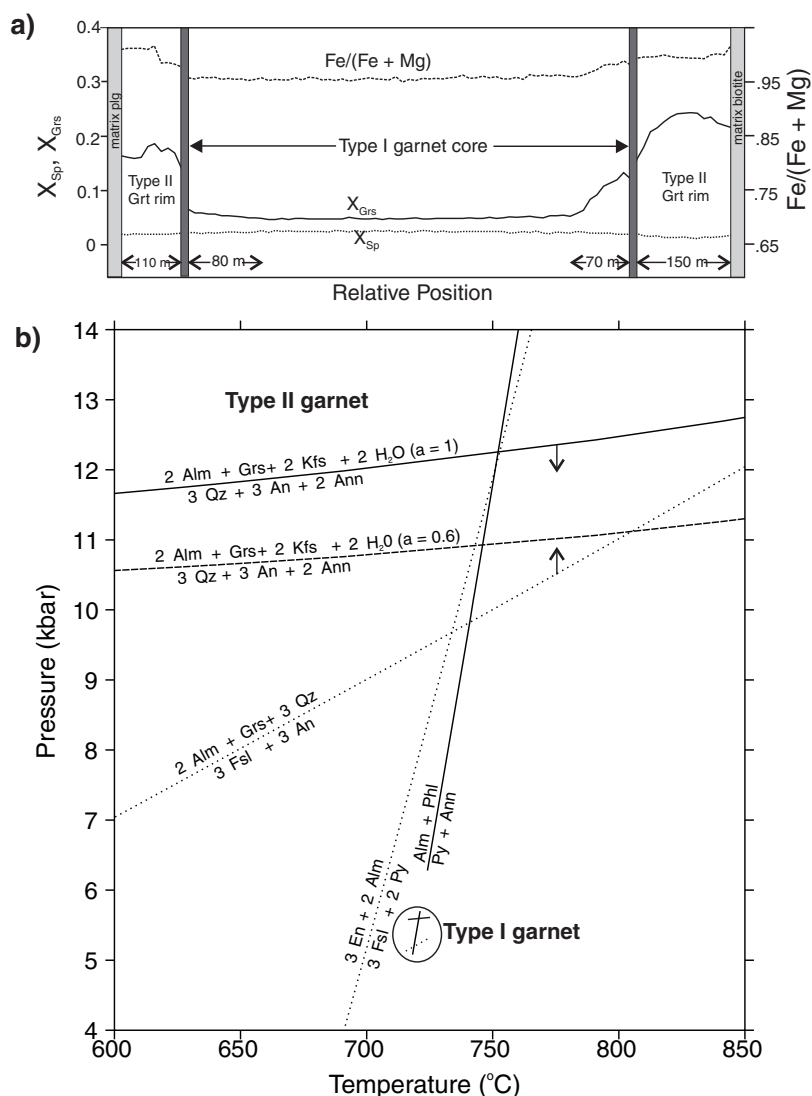


Figure 5.

Chemical and thermobarometric data for sample z6858: **a)** chemical profile across type I and II garnet; **b)** pressure-temperature diagram summarizing equilibria that constrain conditions of formation of type I and II garnet (see Table 1 for more details). Alm, almandine; An, anorthite; Ann, annite; En, enstatite; Grs, grossular; Grt, garnet; Kfs, potassium feldspar; Phl, phlogopite; Py, pyrope; Qz, quartz; X_{Grs} , mole fraction of grossular; X_{Sp} , mole fraction of spessartine.

the outer 70–80 μm of type I garnet (see ‘Interpretation’ section below). The two types of garnet described here are texturally and chemically similar to types I and II garnet within metapelitic rocks of the MacQuoid Lake supracrustal belt (Fig. 2; Berman et al., 2000; Stern and Berman, 2000).

There is very little variation in plagioclase composition, with plagioclase adjacent to type II garnet being slightly more sodic (approx. An_{28}) than matrix plagioclase (approx. An_{31}). Gneissosity-aligned matrix biotite and inclusions armoured within quartz in type I garnet have $Fe/(Fe+Mg)$ ratios of 0.37. Matrix biotite adjacent to type II garnet has $Fe/(Fe+Mg)$ ratios of 0.39–0.42.

Pressure-temperature estimates (Table 1, Fig 5b) were calculated using the TWQ software program (Berman, 1991) with the version 1.02 thermodynamic database (Berman,

1992). Pressure-temperature conditions for type II garnet are constrained between 12.1 kbar and 750°C, and 9.8 kbar and 740°C (Table 1, Fig. 5b), using the maximum X_{Grs} of garnet together with compositions of adjacent, but not touching, matrix plagioclase and biotite. Pressure-temperature conditions for type I garnet are limited to 5.6–5.2 kbar and 730 °C, using the compositions of garnet core, biotite inclusions armoured by quartz, and matrix plagioclase several millimetres removed from the garnet. Because this matrix plagioclase may not have been in equilibrium with type I garnet, the actual equilibration pressure could have been approximately 0.4 kbar higher, reflecting the shift in barometers (Table 1, Fig. 5b) resulting from use of the least calcic plagioclase (mole fraction of anorthite [X_{An}]=0.15) stable at amphibolite facies.

GEOCHRONOLOGY

Sensitive high-resolution ion microprobe (SHRIMP) analytical methods for monazite closely follow those described in Stern and Berman (2000) and Stern and Sanborn (1998). Monazite standard z3345 (1821 Ma), mounted in epoxy along with rock chips of sample z6858, was ground and polished to expose the monazite grains. The beam sizes used were 5–9 μm with primary beam currents of 0.12–0.33 nA O_2^- . The U-Pb calibration error applied was 1.0%.

Monazite is very sparse in sample z6858, with an average of only about 20 grains per thin section examined. Although monazite grains approximately 10–20 μm in size were observed in thin section within type I garnet, none occur in either type of garnet in the rock chip polished for SHRIMP analysis. Of the 13 monazite grains located in this rock chip, four were analyzed. In only one of these grains was a faint internal structure observed with backscattered electron (BSE) or cathodoluminescence imaging.

Five monazite grains were analyzed in situ. Monazite grain 10 is a subhedral, 30 by 15 μm grain, with several small embayments, that occurs interstitially to matrix biotite and

plagioclase. Monazite grain 13 is partially rounded, with several planar crystal faces (Fig 4e), and has a faint internal structure visible with BSE imaging. The elongation of this grain parallel to gneissosity-aligned biotite, with which it is in contact, suggests that this monazite may be syntectonic with respect to the gneissosity. Monazite grain 18 is a 20 by 40 μm grain that is largely idiomorphic except for one irregular boundary in contact with biotite. This grain is enclosed by plagioclase that forms a well-defined leucocratic band; thus, its age likely is synchronous with or predates the formation of the gneissosity. The U-Pb isotopic data for these three monazite grains are indistinguishable (Table 2, Fig. 6), and yield a weighted-mean $^{207}\text{Pb}/^{206}\text{Pb}$ age of 2.54 ± 0.02 Ga (2σ ; mean square of weighted deviates [MSWD] = 0.051).

Two idiomorphic grains, measuring 15 by 40 μm and 20 by 20 μm , occur as part of an aggregate of monazite that partially rims a rounded apatite grain. Given that one grain of the aggregate truncates gneissosity-aligned biotite (Fig. 4f), our interpretation is that these grains provide a minimum age for the gneissosity. The weighted mean $^{207}\text{Pb}/^{206}\text{Pb}$ age of these grains (grains 20.1 and 21.1) is 1.93 ± 0.05 Ga (2σ ; MSWD = 0.113).

Table 2. Sensitive high-resolution ion microprobe (SHRIMP) U-Pb monazite data.

Spot name	U (ppm)	Th (ppm)	Th/U	Pb (ppm)	^{204}Pb (ppb)	$^{204}\text{Pb}/^{206}\text{Pb}$	$\pm^{204}\text{Pb}/^{206}\text{Pb}$	f^{206}	$^{208}\text{Pb}/^{206}\text{Pb}$	$\pm^{208}\text{Pb}/^{206}\text{Pb}$
Lab no. z6858		Field no. 97LA-10-10				UTM = 460100, 6912860 Grid Zone 14				
20.1	6784.49	76030	11.20645	8314	457	2.33E-04	6.47E-05	4.38E-03	3.1006	0.0500
21.1	5505.14	61097	11.09820	6548	36	2.26E-05	2.35E-05	4.30E-04	2.9746	0.0213
10.1	3010.28	90518	30.06951	12157	16	1.31E-05	2.01E-05	2.50E-04	8.7076	0.1127
18.1	3746.23	96110	25.65498	13082	15	1.00E-05	6.23E-05	1.90E-04	7.6519	0.0479
13.1	4599.49	120082	26.10759	16453	31	1.59E-05	1.28E-05	3.00E-04	7.2961	0.0365
Uncertainties reported at one sigma and are calculated by numerical propagation of all known sources of error (Stern and Sanborn, 1998; Stern and Berman, 2000).										
f^{206} refers to mole fraction of total ^{206}Pb that is due to common Pb; data have been corrected for common Pb according to procedures outlined in Stern (1997).										
Conc. = concordance = $100 \times (^{206}\text{Pb}/^{238}\text{U age})/(^{207}\text{Pb}/^{206}\text{Pb age})$										

Table 2. (cont.)

Spot name	$^{206}\text{Pb}/^{238}\text{U}$	$\pm^{206}\text{Pb}/^{238}\text{U}$	$^{207}\text{Pb}/^{235}\text{U}$	$\pm^{207}\text{Pb}/^{235}\text{U}$	$^{207}\text{Pb}/^{206}\text{Pb}$	$\pm^{207}\text{Pb}/^{206}\text{Pb}$	Apparent Ages (Ma)				Conc (%)
							$^{206}\text{Pb}/^{238}\text{U}$	$\pm^{206}\text{Pb}/^{238}\text{U}$	$^{207}\text{Pb}/^{206}\text{Pb}$	$\pm^{207}\text{Pb}/^{206}\text{Pb}$	
Lab no. z6858			Field no. 97LA-10-10				UTM = 460100, 6912860 Grid Zone 14				
20.1	0.336	0.006	5.43	0.17	0.1174	0.0027	1866	30	1916	41	97
21.1	0.336	0.007	5.49	0.15	0.1185	0.0019	1866	33	1933	28	97
10.1	0.472	0.010	10.88	0.30	0.1672	0.0025	2492	45	2529	26	99
18.1	0.457	0.008	10.58	0.21	0.1680	0.0016	2426	33	2538	16	96
13.1	0.488	0.008	11.30	0.22	0.1681	0.0013	2561	35	2538	13	101
Uncertainties reported at one sigma and are calculated by numerical propagation of all known sources of error (Stern and Sanborn, 1998; Stern and Berman, 2000).											
f^{206} refers to mole fraction of total ^{206}Pb that is due to common Pb; data have been corrected for common Pb according to procedures outlined in Stern (1997).											
Conc. = concordance = $100 \times (^{206}\text{Pb}/^{238}\text{U age})/(^{207}\text{Pb}/^{206}\text{Pb age})$											

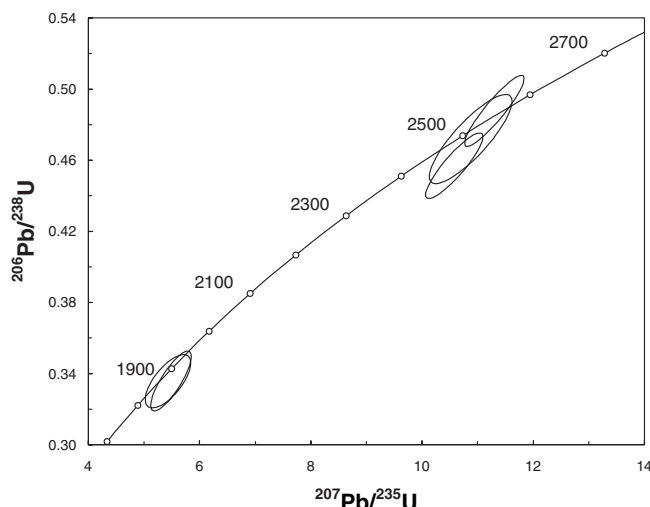


Figure 6. Concordia diagram for metamorphic monazite in sample z6858.

Interpretation of SHRIMP data

The data summarized above indicate that sample z6858 is characterized by two distinct types of garnet that are inferred to be dated by two distinct age populations of monazite. Although no SHRIMP ages were obtained from monazite inclusions in garnet, electron microprobe (CHIME) ages for two monazite inclusions in type I garnet from a thin section of the same rock yielded an average age of 2.55 Ga. The idiomorphic nature of these grains (e.g. Fig. 4b) suggests synchronous growth of type I garnet (Stern and Berman, 2000). The CHIME data also constrain the gneissosity enveloping the type I garnet host of the dated monazite (Fig. 4b) to be ≤ 2.55 Ga, consistent with the syntectonic interpretation of the 2.54 Ga SHRIMP age of monazite grain 13 (*see above*). These conclusions agree well with the 2.55 ± 0.02 Ga age of type I garnet and the enveloping regional S_2 fabric determined at MacQuoid Lake (Stern and Berman, 2000).

The age of type II garnet in sample z6858 cannot be defined unambiguously. Given the parallel between two distinct garnet types and monazite ages, the type II garnet is inferred to be dated by the $ca. 1.93 \pm 0.05$ Ga monazite, based on several lines of reasoning. First, the growth of both type II garnet (Fig. 4c, 4d) and 1.93 Ga monazite (Fig. 4f) appears to be post-tectonic with respect to the gneissosity in sample z6858. Second, 2.19 Ga diabase dykes in the Parker Lake–MacQuoid Lake belt contain post-tectonic coronitic garnet that records pressure-temperature conditions identical to those of type II garnet in the surrounding metasedimentary rocks (Berman et al., 2000), demonstrating that at least the Parker Lake–MacQuoid Lake area experienced high-pressure, static metamorphism after 2.19 Ga. Third, the elevated CaO concentrations that occur around several fractures internal to type I garnet (*see above*) suggest that high-CaO garnet formed during a high-pressure event that occurred after *ca.* 2.5 Ga type I garnet cooling and uplift. The CaO decrease at the extreme rim of type I garnet is interpreted to

reflect this uplift, and the increasing CaO toward the centre of type II garnet to reflect thickening during growth at *ca.* 1.9 Ga. It should be noted, however, that the present data do not exclude the possibility that type II garnet grew during the same *ca.* 2.5 Ga event as type I garnet. This possibility, however, requires that the fractures in type I garnet formed at elevated pressure-temperature prior to type II garnet growth during thickening.

CONCLUSIONS

The geochronological data reported here for domain 2 at Angikuni Lake indicate metamorphic monazite growth at *ca.* 2.54 and 1.9 Ga that is associated, respectively, with distinct episodes of dynamic, low-pressure and static, high-pressure metamorphism. The new results demonstrate that a region of 2.56–2.5 Ga, high-grade metamorphism and associated deformation extends approximately 400 km through the northwestern Hearne domain from Chesterfield Inlet to at least as far southwest as the Angikuni Lake area (Fig. 2). Recent work in the Yathkyed Lake (MacLachlan et al., 2000) and MacQuoid Lake (Tella et al., 2001; Ryan et al., 2000; S. Hanmer et al., unpub. data, 2002) supracrustal belts has documented that the *ca.* 2.5 Ga event involved regional-scale, southeast-vergent thrust tectonics. The metamorphic signature of Neoproterozoic thrust thickening in the Parker Lake–MacQuoid Lake area (Fig. 2) is an increase in CaO within the outer 60–120 μ m rim of type I garnet (R.G. Berman, unpub. data, 2002). As chemical zoning in type I garnet in domain 2 at Angikuni Lake is remarkably similar, it appears that this region experienced thickening of a similar style. The authors suggest that this event was associated with tectonic burial beneath a southeast-directed thrust nappe that forms part of the hanging wall of the Tyrell shear zone near Yathkyed Lake (MacLachlan et al., 2000).

ACKNOWLEDGMENTS

We are very grateful to Maggie Currie for her patient drafting and sharp-eyed monazite hunting; Pat Hunt for assistance with the SEM; Deborah Lemkow for troubleshooting graphics problems; and Katherine Venance for providing microprobe analyses. The help of Richard Stern and Natalie Morisset was instrumental in acquiring the SHRIMP data. We appreciate very helpful reviews provided by Chris Carson, Simon Hanmer, and Richard Stern. The work described in this report was carried out as part of geochronology project P80.

REFERENCES

- Ansdell, K.M., Lucas, S.B., Connors, K., and Stern, R.A. 1995: Kiseeynew metasedimentary gneiss belt, Trans-Hudson Orogen (Canada): back-arc origin and collisional inversion; *Geology*, v. 23, p. 1039–1043.
- Aspler, L.B., Chiarenzelli, J. R., Cousens, B.L., and Valentino, D. 1999: Precambrian geology, northern Angikuni Lake, and a transect across the Snowbird tectonic zone, western Angikuni Lake, Northwest Territories (Nunavut); in *Current Research 1999-C*; Geological Survey of Canada, p. 107–118.

- Berman, R.G.**
 1991: Thermobarometry using multiequilibrium calculations: a new technique with petrological applications; *Canadian Mineralogist*, v. 29, p. 833–856.
 1992: Thermobarometry with estimation of equilibration state (TWEQU): an IBM-compatible software package; Geological Survey of Canada, Open File 2534.
- Berman, R.G. and Bostock, H.H.**
 1997: Metamorphism in the northern Taltson magmatic zone, Northwest Territories; *Canadian Mineralogist*, v. 35, p. 1069–1092.
- Berman, R.G., Ryan, J.J., Tella, S., Sanborn-Barrie, M., Stern, R.A., Aspler, L., Hanmer, S., and Davis, W.**
 2000: The case of multiple metamorphic events in the western Churchill Province: evidence from linked thermobarometric and in-situ SHRIMP data, and jury deliberations; *in* GeoCanada 2000; Geological Association of Canada–Mineralogical Association of Canada, Joint Annual Meeting, Calgary, CD-ROM, abstract 836.
- Davidson, A.**
 1972: The Churchill Province; *in* Variations in Tectonic Styles in Canada, (ed.) R.A. Price and R.J.W. Douglas; Geological Association of Canada, Special Paper 11, p. 381–433.
- Davis, W.J., Hanmer, S., Aspler, L., Sandeman, H., Tella, S., Zaleski, E., Relf, C., Ryan, J., Berman, R., and MacLachlan, K.**
 2000: Regional differences in the Neoproterozoic crustal evolution of the western Churchill Province: can we make sense of it? *in* GeoCanada 2000; Geological Association of Canada–Mineralogical Association of Canada, Joint Annual Meeting, Calgary, CD-ROM, abstract 864.
- Hoffman, P.F.**
 1990: Subdivision of the Churchill Province and extent of the Trans-Hudson Orogen; *in* The Early Proterozoic Trans-Hudson Orogen of North America, (ed.) J.F. Lewry and M.R. Stauffer; Geological Association of Canada, Special Paper 37, p. 15–39.
- MacLachlan, K., Relf, C., and Davis, W.J.**
 2000: U/Pb geochronological constraints on structures controlling distribution of tectonothermal domains, Yathkyed Lake area, western Churchill Province; *in* GeoCanada 2000; Geological Association of Canada–Mineralogical Association of Canada, Joint Annual Meeting, Calgary, CD-ROM, abstract 751.
- Mills, A.**
 2001: Tectonic evolution of the Uvauk complex, Churchill Province, Nunavut Territory, Canada; M.Sc. thesis, Carleton University, Ottawa, Ontario.
- Paul, D., Hanmer, S., Tella, S., Peterson, T.D., and LeCheminant, A.N.**
 in press: Compilation bedrock geology of part of the western Churchill Province, Nunavut; Geological Survey of Canada, Open File 4236, map at 1:1000 000 scale.
- Sanborn-Barrie, M., Carr, S.D., and Thériault, R.**
 2001: Geochronological constraints on metamorphism, magmatism, and exhumation of deep-crustal rocks of the Kramanitar Complex, with implications for the Paleoproterozoic evolution of the Archean western Churchill Province, Canada; *Contributions to Mineralogy and Petrology*, v. 141, p. 592–612.
- Ryan, J.J., Davis, W., Berman, R., Sandeman, H., Hanmer, S., and Tella, S.**
 2000: 2.5 Ga granulite-facies activity and post-1.9 Ga low-grade reactivation along the Big lake shear zone, MacQuoid–Gibson lakes area (Nunavut): a fundamental boundary in the western Churchill Province; *in* GeoCanada 2000; Geological Association of Canada–Mineralogical Association of Canada, Joint Annual Meeting, Calgary, CD-ROM, abstract 924.
- Stern, R.A.**
 1997: The GSC sensitive high resolution ion microprobe (SHRIMP): analytical techniques of zircon U–Th–Pb age determinations and performance evaluation; *in* Radiogenic Age and Isotopic Studies: Report 10; Geological Survey of Canada, Current Research 1997-F, p. 1–31.
- Stern, R.A. and Berman, R.G.**
 2000: Monazite U–Pb and Th–Pb geochronology by ion microprobe, with an application to in situ dating of an Archean metasedimentary rock; *Chemical Geology*, v. 172, p. 113–130.
- Stern, R.A. and Sanborn, N.**
 1998: Monazite U–Pb and Th–Pb geochronology by high-resolution secondary ion mass spectrometry; *in* Radiogenic Age and Isotopic Studies: Report 11; Geological Survey of Canada, Current Research 1998-F, p. 1–18.
- Stockwell, C.H.**
 1982: Proposals for time classification and correlation of Precambrian rocks and events in Canada and adjacent areas of the Canadian Shield, Part I: a time classification of Precambrian rocks and events; Geological Survey of Canada, Paper 80-19, 135 p.
- Tella, S., Hanmer, S., Sandeman, H.A., Ryan, J.J., Mills, A., Davis, W.J., Berman, R.G., Wilkinson, L., and Kerswill, J.A.**
 2001: Geology, MacQuoid Lake–Gibson Lake–Akunak Bay area, Nunavut; Geological Survey of Canada, Map 2008A, scale 1:100 000.
- Tella, S., Schau, M., Roddick, J.C., and Mader, U.**
 1994: Significance of juxtaposed mid-crustal mylonite zones of contrasting ages, Uvauk Complex, central Churchill Province, District of Keewatin, N.W.T., Canada; *Geological Society of America, Abstracts with Programs*, v. 26, p. 135.
- Wheeler, J., Hoffman, P., Card, K., Davidson, A., Sanford, B., Okulitch, A., and Roest, W.**
 1996: Geological map of Canada; Geological Survey of Canada, Map 1860A, scale 1:5 000 000.

Geological Survey of Canada Project 970006